Studies of hadronic interactions at ultra-high energies with the Pierre Auger Observatory

D. Garcia-Gamez

▶ **To cite this version:**

D. Garcia-Gamez. Studies of hadronic interactions at ultra-high energies with the Pierre Auger Observatory. XLVIIth Rencontres de Moriond - QCD AND HIGH ENERGY INTERACTIONS, Mar 2012, La Thuile, Italy. pp.307-312. in2p3-00679927

HAL Id: in2p3-00679927
https://hal.in2p3.fr/in2p3-00679927

Submitted on 14 Dec 2012

HAL is a multi-disciplinary open access archive for the deposit and dissemination of scientific research documents, whether they are published or not. The documents may come from teaching and research institutions in France or abroad, or from public or private research centers.

L'archive ouverte pluridisciplinaire **HAL**, est destinée au dépôt et à la diffusion de documents scientifiques de niveau recherche, publiés ou non, émanant des établissements d'enseignement et de recherche français ou étrangers, des laboratoires publics ou privés.

STUDIES OF HADRONIC INTERACTIONS AT ULTRA-HIGH ENERGIES WITH THE PIERRE AUGER OBSERVATORY

DIEGO GARCIA-GAMEZ[1] FOR THE PIERRE AUGER COLLABORATION[2]
[1] *Laboratoire de l'Accélérateur linéaire (LAL), Université Paris 11, CNRS-IN2P3, Orsay, France*
[2] *Observatorio Pierre Auger, Av. San Martin Norte 304, 5613 Malargüe, Argentina*
(Full author list: http://www.auger.org/archive/authors_2012_01.html)

The hybrid design of the Pierre Auger Observatory allows one to measure the longitudinal profile of ultra-high energy air showers and the depth at which the shower reaches its maximum size, $X_{\max}$. It also provides a record of the shower front by sampling the secondary particles at ground level. These measurements give a variety of independent experimental observables with information about the nature of the primary particle and its interactions. In this contribution we present a comparison of our mass sensitive observables with the prediction of different hadronic interaction models. Furthermore we show how the analysis of the tail of the distribution of $X_{\max}$ allows one to estimate the proton-air cross-section for particle production at center-of-mass energies of 57 TeV.

1 Introduction

The Pierre Auger Observatory is the largest cosmic ray observatory ever built. It was conceived to study the properties of ultra-high energy cosmic rays (UHECR). It is a hybrid detector that combines both surface and fluorescence detectors at the same site [1]. The Surface Detector (SD) [2] consists of a triangular grid of over 1600 water Cherenkov detectors spaced 1.5 km and covering a surface of about 3000 km^2. The purpose of these detectors is to measure the density of particles at the ground. The Fluorescence Detector (FD) [3,4] consists of 27 telescopes placed at four sites surrounding the SD and looking to the atmosphere. Their aim is to collect the UV light track emitted by the de-excitation of air molecules. The detection of this radiation is only possible during dark nights without moon. That results in a small duty cycle of about 13 %, which contrasts with the nearly 100 % of the SD. As the atmosphere is where extensive air showers (EAS) develop, a good knowledge of its state is of great importance for an experiment like the Pierre Auger Observatory. In any FD measurement, the atmosphere is the medium where emission and transmission of recorded light occur. The particle density at ground sampled by the SD, particularly the electromagnetic component, is also sensitive to the amount of matter traversed. Hence, fluctuations in the atmospheric conditions have an effect over both the longitudinal [5] and the lateral [6] developments of the showers. Different monitoring devices are placed at the observatory site to record atmospheric conditions. This is crucial to be able to understand the functioning of the detector and correct the different measurements.

The goal of any UHECR detector is to measure the development of EAS. This development is extremely sensitive to the hadronic interaction properties at ultra-high energies. Although the results coming from LHC will be of great help, the range of energies that governs the features of these showers is not accessible by any current accelerator. Therefore the different models are

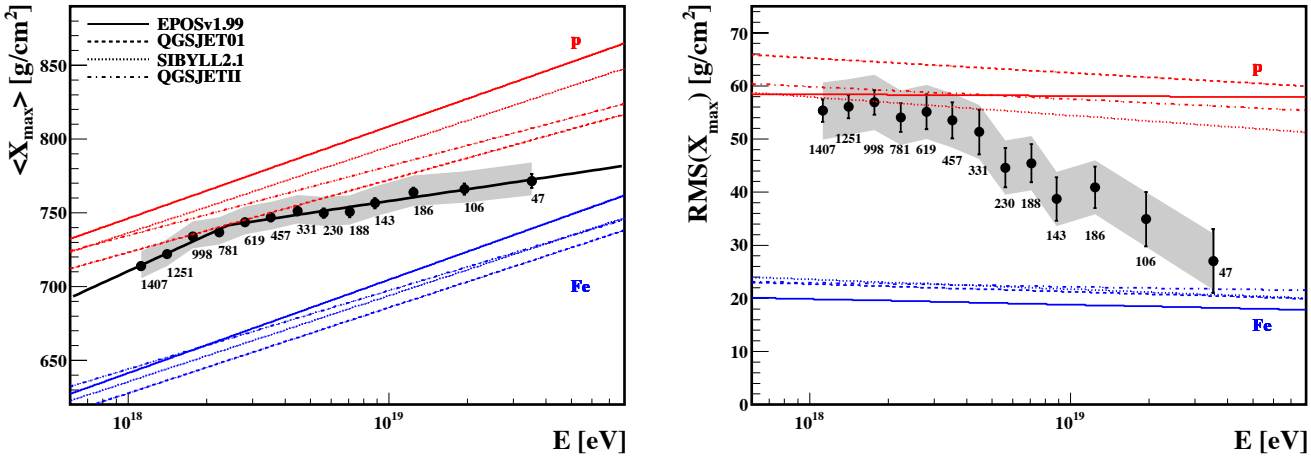

Figure 1: $\langle X_{\rm max}\rangle$ (left) and RMS($X_{\rm max}$) (right) as a function of the energy. The number of real data events in each energy bin is indicated. The predictions for proton and iron, following different hadronic models, are shown as well. The shaded region represents the systematic uncertainties.

built over different extrapolations and approximations [7,8,9]. Differences in multi-particle production models are directly reflected in shower observables like $X_{\rm max}$ and the number of muons at ground level. Other hadronic interaction features like the particle production cross-section, elasticity or charge-ratio (fraction of particles going into the electromagnetic (EM) cascade) have also their own impact on the different shower observables. They have been studied in detail in [10]. This interconnection allows the study of hadronic interactions at ultra-high energies using cosmic ray data. The main problem for this kind of analysis is that the cosmic ray composition is unknown at these energies. Furthermore, the mass of the primary particles can only be determined by comparing air shower observables with simulations. All this, along with their origin and mechanisms of acceleration, is the complex cosmic ray puzzle that experiments like the Pierre Auger Observatory try to solve. In Sec. 2 we describe the main observables and analysis carried out by the Auger collaboration to infer the mass of the primary particles measured with both the FD and the SD. The measurement of the proton-air cross-section from the tail of the $X_{\rm max}$ distribution is discussed in Sec. 3. We finish this document (in Sec. 4) with different studies that highlight the muon deficit found in simulations when compared with real data.

2 Measurements of the Longitudinal Shower Development

2.1 Fluorescence Detector Measurements

With the fluorescence detector of the Pierre Auger Observatory it is possible to measure the longitudinal development of cosmic rays in the atmosphere. The preferred observable used for composition studies is the depth of the maximum in the shower development, $X_{\rm max}$. A simple way to understand the sensitivity of this variable to the mass of the primary particle is the superposition model. It states that the interaction of a nucleus with mass A and energy E can be seen as the superposition of A nucleons interacting with an energy E/A. All this, in the framework of the extended Heitler model [11,12], leads to the following expresion where the mass dependence is shown:

$$\langle X^A_{\rm max}\rangle = c + D_p \ln(E/A). \quad (1)$$

The elongation rate $D_p = dX_{\rm max}/dlnE$ and the parameter c contain the dependency on the hadronic interaction properties. Also the fluctuations in $X_{\rm max}$ carry information about the pri-

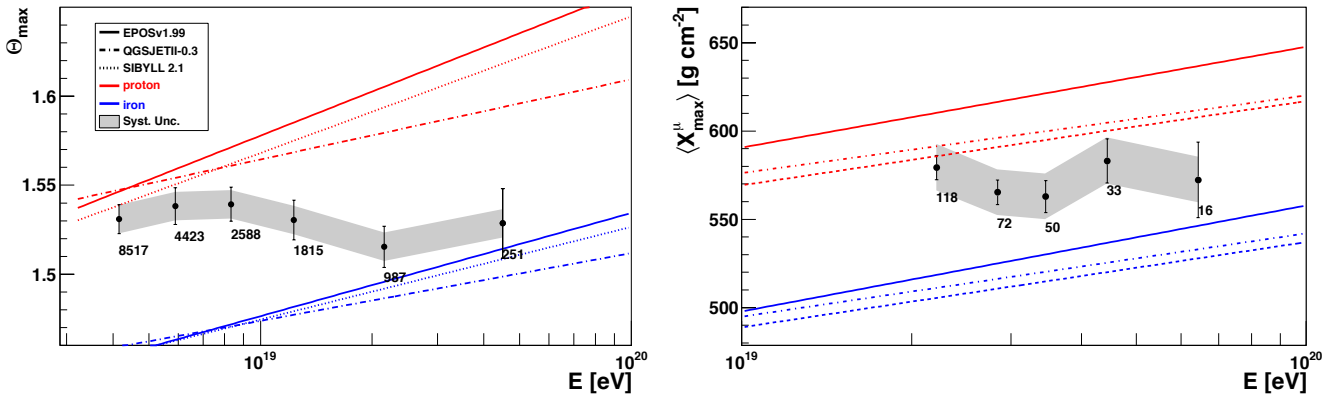

Figure 2: The azimuthal rise-time asymmetry Θ_{max} (left panel) and $\langle X^{\mu}_{\rm max}\rangle$ (right panel) as a function of the energy. The number of events in each bin is indicated.

mary particles. They are supposed to be smaller for heavy than for light nuclei.
When we analyse real data we have to compare them with simulations. Given that accelerator data do not cover the energy range of the first interactions produced in the cascade development, models must rely in theoretical extrapolations. Differences between them are often used as an estimation of the systematic uncertainties due to the lack of knowledge in the hadronic interactions at ultra-high energies.
The measurement of the longitudinal profile of the energy deposited in the atmosphere with the Pierre Auger Observatory is described in [14]. Only hybrid events (showers measured with the FD and at least one SD station in coincidence) are considered in this analysis, to provide an accurate reconstruction of the geometry. To ensure a good $X_{\rm max}$ resolution and an unbiased mean measurement (not undersampling the tails of the $X_{\rm max}$ distributions) different set of cuts are applied over the data sample [15]. Figure 1 shows the results for the $\langle X_{\rm max}\rangle$ analysis. Along with the predictions for different hadronic interaction models and primaries, the mean values (left panel) and the RMS (right panel) of the $X_{\rm max}$ distributions are shown as a function of the primary energy. The elongation rate is well described with a linear fit broken at $\log(\mathrm{E/eV})=18.38^{+0.07}_{-0.17}$ [16]. This change in the elongation rate can be interpreted as a transition from lighter to heavier primaries as the energy increases. The values for the $X_{\rm max}$ fluctuations shown in Figure 1 have been corrected by the detector resolution [16]. Again, assuming that the hadronic interaction properties do not change much within the observed energy range, this result is an independent signature of an increasing average mass of the primary particles with energy. The compatibility of the Auger results for $\langle X_{\rm max}\rangle$ and RMS($X_{\rm max}$) with different hadronic interaction models has been studied in [17]. A direct comparison between the shape of the measured $X_{\rm max}$ distributions with different hadronic models and primaries is discussed in [16].

2.2 Surface Detector Measurements

In the development of EAS, the atmosphere acts as a huge calorimeter absorbing part of the EM component in its path to ground. This means that the number of these particles at ground relates with the depth of the shower maximum. Furthermore, the arrival time for the muon component is earlier than for EM particles, since they travel in almost straight lines with smaller multiple scattering. Based on this, it is possible to find observables relating to primary particle composition in the time structure of particles at ground, recorded by the water Cherenkov detectors of the Pierre Auger Observatory.

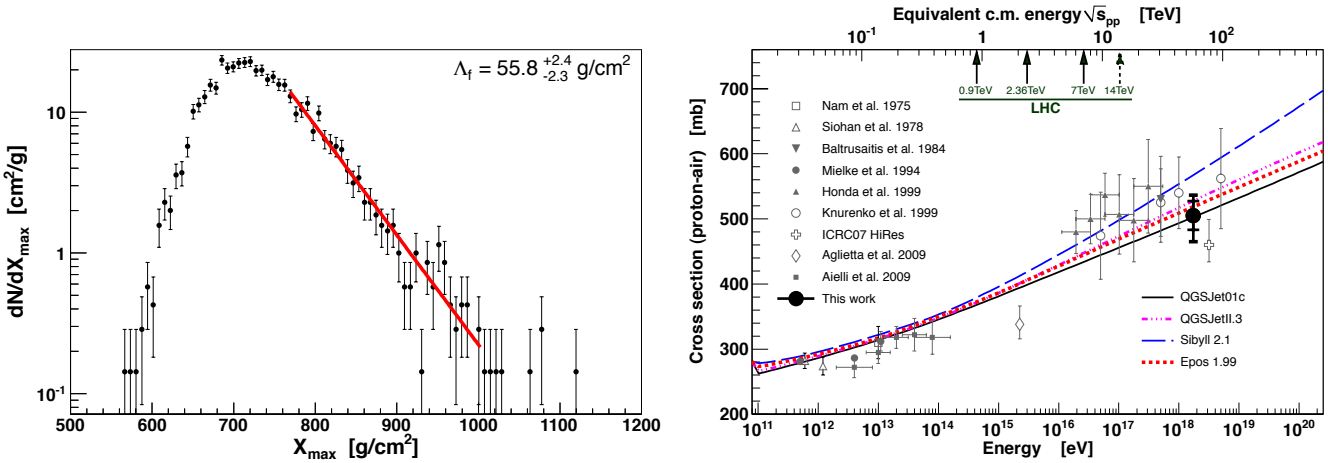

Figure 3: Left: Unbinned likelihood fit of the tail of X_{max} distribution in the energy interval 10^{18}-$10^{18.5}$ eV. Right: Proton-air cross-section measured by Auger and other cosmic ray experiments along with different model predictions.

The so called rise-time of the signal (the time to go from the 10% to the 50% of the total integrated signal), $t_{1/2}$, is a measurement of the muon to electron ratio in a SD detector. It depends on the primary mass, the zenith angle θ and the distance to the shower axis r. The azimuthal asymmetry of $t_{1/2}$ for non vertical events carries information about the longitudinal development of the shower [18]. The maximum of this asymmetry, Θ_{max}, has been used to study the composition of cosmic rays.

Using signals dominated by muons (in inclined events and far from the shower core) it is possible to reconstruct the muon production depth distribution (MPD) [19]. In this technique the arrival times of the muons are converted into their production distances along the shower axis assuming they travel undeflected from birth until reaching the ground. These distributions carry information about the hadronic longitudinal development of the shower. The maximum $X^{\mu}_{\rm max}$ of these profiles is strongly correlated with the depth of the first interaction X_1, and $X_{\rm max}$, so it is also sensitive to the nature of primary particles.

Figure 2 shows the values of Θ_{max} and $\langle X^{\mu}_{\rm max}\rangle$ as a function of the energy. Both results are compatible with showers that develop earlier than pure proton showers in the highest energy region.

3 Proton-air cross-section

The Pierre Auger Collaboration has measured the proton-air cross-section, σ_{p-air}, for particle production at ultra-high energies using hybrid data. This cross-section is directly related with the exponential distribution of X_1. The strong correlation between X_1 and $X_{\rm max}$ makes the tail of the $X_{\rm max}$ distribution still sensitive to the proton-air cross-section. This quality was first exploited for this purpose by the Fly's Eye Collaboration [20]. The idea is to fit the deep tail of the $X_{\rm max}$ distribution with an exponential function and use the slope as an estimator of σ_{p-air}. The translation to a cross-section is done using Monte Carlo simulations with a consistent rescaling of the original cross-section to reproduce the value of the measurement [21].

One of the main difficulties in this analysis is the poor knowledge of mass composition at these energies. The tail of $X_{\rm max}$ distribution is supposed to be proton-rich as protons are the most penetrating nuclei. However we cannot exclude the presence of other primaries, mainly helium and photons. The possible photon impact is almost under control thanks to the strong limits reported on the photon fraction in Auger data [22]. But no limit exists on the helium fraction of cosmic rays at these energies. This lack of knowledge translates into the main contribution to

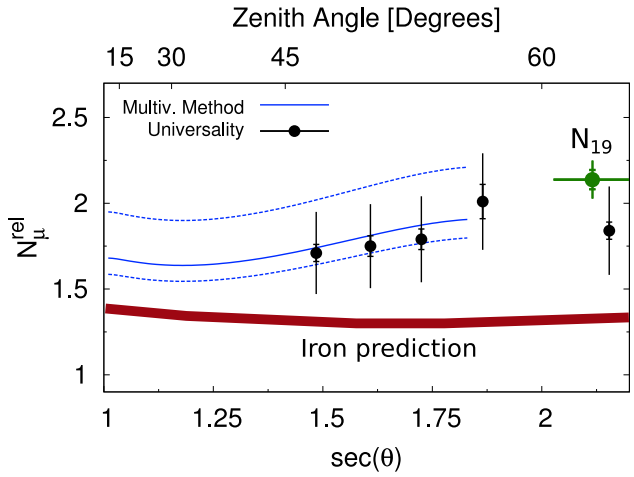

Figure 4: Data from the Pierre Auger Observatory showing the measured number of muons at 1000 m from the shower axis and 10^{19} eV relative to the predictions of the hadronic model QGSJETII for proton initiated showers (N_μ^{rel}) as a function of the zenith angle. The figure shows the results derived from the multivariate, shower universality and inclined events (N_{19}) methods. The result for pure iron simulations is also shown.

the systematic uncertainty of this measurement. Figure 3 left panel shows the selected $X_{\max}$ distribution and the fit of its exponential tail. Only events with E$\in [10^{18}eV, 10^{18.5}eV]$ are used in this analysis, resulting in an averaged center-of-mass energy of $\sqrt{s} = 57$ TeV. If we neglect the possible presence of helium in our data sample, then the measured proton-air cross-section is

$$\sigma_{p-air} = (505 \pm 22_{stat} \pm (^{+20}_{-15})_{sys})mb. \quad (2)$$

Using simulations we find that a 50 % fraction of helium would reduce the actual value of the measured cross-section by 80 mb [21]. In Figure 3, right panel, we show the measured σ_{p-air} together with different model predictions and other measurements derived from cosmic ray data. Our result favors a moderately slow rise of the cross-section towards higher energies.

4 Muon shower content

A good description of shower data is essential to draw the right conclusions when comparing the measurements with simulations. As mentioned in the text, the number of muons at ground depends on several properties of hadronic interactions [10], becoming a powerful tool in the difficult task of validate the various existing models. Different methods have been developed to derive the fraction of the signals, collected by the surface detectors, coming from the muonic or the electromagnetic component of the shower using the Auger data. Some of these methods are based on the different time structure showed by both components [23]. Muons typically deposit more energy in the water Cherenkov detectors than electrons and photons, producing spikes over the smoother EM contribution in the signals. The multivariate method exploits this feature in the time traces to build an estimator correlated with the number of muons. The universality method uses a recently found shower universality property which relates the muon to electromagnetic signal ratio with the maximum in the shower development [24]. This property can be described by a simple parameterization for showers with zenith angle between 45° and 65°. Then, for hybrid events, this method derives the muonic signal in a SD detector from the shower maximum depth and the total signal. The most direct way to investigate the muon content of cosmic ray showers is by studying very inclined events, where the dominant particles at ground are muons

because most of the electrons and photons have been absorbed in the atmosphere[25]. Using hybrid inclined events, the measured shower size N_{19}, which is a muon estimator itself, can be calibrated with the calorimetric energy reconstructed by the FD. This calibration procedure can be used to obtain the number of muons as a function of energy. A summary of the results obtained when we apply these methods to real data is presented in Figure 4. It shows the estimated number of muons at 1000 m in data relative to the predictions of simulations using the hadronic model QGSJETII[7] with proton primaries. In view of this figure, the considered simulations are found to present underestimations of the muon fraction at ground level for the events measured with the Pierre Auger Observatory. The observed relative excess is angle dependent, growing from about 1.6 [23], at the lower zenith angles, to more than 2 [25], for the more inclined events. Understanding this discrepancy is critical to an appropriate interpretation of cosmic ray data. Different efforts are focused on that. For example, it has been recently demonstrated that a larger baryon anti-baryon pair production yields to a higher number of low energy muons[8].

Acknowledgments

This work was supported by the ANR-2010-COSI-002 grant of the French National Research Agency.

References

1. J. Abraham *et al*, (Pierre Auger Collab.), *Nucl. Instr. and Meth. A*, **523**, 50-95, (2004)
2. J. Abraham *et al*, (Pierre Auger Collab.), *Nucl. Instr. and Meth. A*, **613**, 29-39, (2010)
3. J. Abraham *et al*, (Pierre Auger Collab.), *Nucl. Instr. and Meth. A*, **620**, 2-3, (2010)
4. H.-J. Mathes *et al*, (Pierre Auger Collab.), *Proc. 32nd ICRC*, (2011), arXiv:1107.4807v1
5. J. Abraham *et al*, (Pierre Auger Collab.), *Astropart. Phys.* **33**, 108-129, (2010)
6. J. Abraham *et al*, (Pierre Auger Collab.), *Astropart. Phys.* **32**, 88-99, (2009)
7. S.S Ostapchenko, *Nucl. Phys.* B **151**, 143-146 (2006)
8. T. Pierog and K. Werner, *Phys. Rev. Lett.* **101**, 171101 (2008)
9. E.J. Ahn *et al*, *Phys. Rev.* D **80**, 094003 (2009)
10. R. Ulrich *et al*, *Phys. Rev.* D **83**, 054026 (2011)
11. W. Heitler, *Oxford University Press*, (1954)
12. J. Matthews, *Astropart. Phys.* **22**, 387, (2005)
13. N.N. Kalmykov and S.S. Ostapchenko, *Phys. Atom. Nucl.* **56**, 346-353 (1993)
14. J. Abraham *et al*, (Pierre Auger Collab.), *Phys. Rev. Lett.* **104**, 091101 (2010)
15. M. Unger *et al*, (Pierre Auger Collab.), *Nucl. Phys. B Proc. Suppl.* **190**, 240, (2009)
16. P. Facal *et al*, (Pierre Auger Collab.), *Proc. 32nd ICRC*, (2011), arXiv:1107.4804v1
17. Karl-Heinz Kampert and Michael Unger, *Astropart. Phys.* **35**, 660-678, (2012)
18. M.T. Dova *et al*, *Astropart. Phys.* **31**, 312-319, (2009)
19. D. Garcia-Gamez *et al*, (Pierre Auger Collab.), *Proc. 32nd ICRC*, (2011), arXiv:1107.4804v1
20. R. Ellsworth *et al*, *Phys. Rev.* D **26**, 336 (1982)
21. R. Ulrich *et al*, (Pierre Auger Collab.), *Proc. 32nd ICRC*, (2011), arXiv:1107.4804v1
22. M. Settimo *et al*, (Pierre Auger Collab.), *Proc. 32nd ICRC*, (2011), arXiv:1107.4805v1
23. J. Allen *et al*, (Pierre Auger Collab.), *Proc. 32nd ICRC*, (2011), arXiv:1107.4804v1
24. A. Yushkov *et al*, *Phys. Rev.* D **81**, 123004 (2010)
25. G. Rodriguez *et al*, (Pierre Auger Collab.), *Proc. 32nd ICRC*, (2011), arXiv:1107.4809v1